Journal of Sound and Vibration 332 (2013) 3646–3654

Contents lists available at SciVerse ScienceDirect

Journal of Sound and Vibration

journal homepage: www.elsevier.com/locate/jsvi

On the linear elastic, isotropic modeling of poroelastic distributed vibration absorbers at low frequencies

R.L. Harne *

Department of Mechanical Engineering, Virginia Polytechnic Institute and State University, 151 Durham Hall (MC 0238), Blacksburg, VA 24061, USA

ARTICLE INFO

Article history:
Received 6 March 2012
Received in revised form
27 January 2013
Accepted 1 February 2013
Handling Editor: D.J. Wagg
Available online 1 March 2013

ABSTRACT

Several past works have considered a passive vibration absorber device utilizing distributed mass and spring layers. The thickness of the poroelastic foam spring and the area density of the mass layer are modified to achieve a target natural frequency of the device while the foam itself provides adequate dissipation of energy as the mass dynamically compresses it at resonance. A model of the device earlier developed is briefly reviewed and validated by new experiments. The dependence of the absorber natural frequency and damping on the poroelastic spring thickness is observed in detail and is found to be consistent with past work on poroelastic material elastic characteristics outside of the linear dynamic regime. The results set a practical limit on the applicability of linearity assumptions in the present modeling of the distributed poroelastic vibration absorbers and thus determine a design parameter range for which the computationally efficient model is accurate.

1. Introduction

Vibration control of structures or surfaces is a long-standing concern. Due to the reliability of performance and limited required maintenance, passive vibration control treatments are frequently the preferred remedy. Mid to high frequency attenuation has oftentimes been achieved using constraining layer damping (CLD) treatments due to the shorter flexural wavelengths of the structures and therefore greater induced shear stress within the damping material between the structure and constraining layer. Many analyses and experiments have considered the design and optimization of such damping solutions [1–7]. However, these treatments are ineffective at low frequencies and the classical dynamic vibration absorber (DVA), tuned for a target structural mode, is an alternative solution in this event.

The DVA has taken many forms: fluid-filled tanks [8–10], point mass–spring–dampers [11–13], pendulums or cantilevered beams [14,15], to name a few. The modeling and characterization of such devices has followed suit with a variety of works focusing on either single-mode attenuation [16–18] or broadband performance [19–22]. Recently, focus has been put on distributed devices composed of poroelastic foam with an embedded piezoelectric film for actuation purposes, termed smart foam [23–25]. The embedded piezoelectric film supplies a controlled distributed force against the flexural vibration of the host structure to improve low frequency attenuation. These devices have also been considered with a distributed top mass layer (a plate) which collectively yield both the effects of a passive distributed vibration absorber and an active device [26–28].

* Tel.: +1 540 231 4162.
E-mail addresses: rharne@umich.edu, rharne@vt.edu

0022-460X/$ - see front matter © 2013 Elsevier Ltd. All rights reserved.
http://dx.doi.org/10.1016/j.jsv.2013.02.002

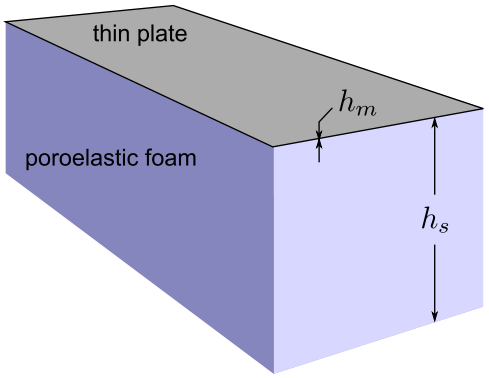

Fig. 1. Schematic of the poroelastic DVA.

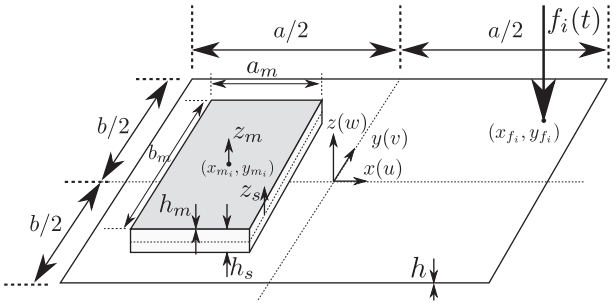

Fig. 2. Model geometries of excited base plate and attached poroelastic DVAs.

The latter passive device is the focus of the present work, Fig. 1. A thin plate is attached to a poroelastic material of the same planar dimensions; this device thereafter exhibits a single degree-of-freedom (SDOF) natural frequency which is a function of the foam mechanical properties and geometry and top plate area density. Using common acoustic foam materials, *e.g.* melamine or polyurethane, and thin mass layers, *e.g.* $h_m < 2$ mm, these devices can be easily tuned to have SDOF resonances < 200 Hz and be a very lightweight embodiment of the DVA to passively attenuate vibrating surfaces, which oftentimes have modal resonances in this frequency range. The use of poroelastic foam also serves to provide for adequate dissipation of energy as the elastic loss factor of such foams is on the order of 10 percent [29–31].

The poroelastic DVA has been considered in detail regarding optimization for passive and active control of an externally excited plate [26]. Dynamics resulting from moderate compression of the poroelastic foam (*i.e.* slightly greater strain than the linear regime) were observed but not explored in great detail. The experimental results showed a hardening spring effect of the foam for moderate compression levels which is inconsistent with other literature on the mechanical properties of poroelastic foams [29,30,32].

The objectives of this paper are to revisit the continuum domain model proposed in Ref. [26], explore the effect of moderate dynamic compression levels via further analyses and experiments, and draw conclusions on the limits of the model's practical applicability due to linear elasticity assumptions. The computational simplicity of the model is a substantial improvement to three-dimensional finite element (FE) analysis but it is important to understand the influence of the modeling assumptions on the range of utility for such analysis. An overview of the analytical model is initially provided; this model allows for the prediction of the dynamics of an externally excited host plate to which a number of poroelastic DVAs are attached. Predictions of foam DVA SDOF resonance dynamics are compared against new experimental data. The absorber natural frequency and damping are considered closely to determine the influence of changing DVA foam spring thickness, and consequently the percentage of dynamic compression. The observations allow for the determination of a range of design parameters for which the model is accurate and therefore serves as the most efficient solution for prediction of vibration control performance when implementing poroelastic DVAs on vibrating structures.

2. Modeling overview

For conciseness, only an overview of the model is provided here since the complete derivation is given in Ref. [26]. The coupled dynamic system of the model is shown in Fig. 2. Poroelastic DVAs are attached to a thin host plate which is excited by one or more point forces. The base plate and the top mass layer of the DVAs are considered to be thin, Love–Kirchhoff plates. The poroelastic spring is considered to be a thick, isotropic plate and acoustical features are neglected. It is noted

that Ref. [26] considers the transverse, *i.e.* z-axis, stiffness of the melamine foam to be slightly different than the in-plane stiffnesses which is consistent to the variation of in-plane to transverse stiffnesses observed in other literature [29]. However, this modification is presently unnecessary given that good agreement is found between the isotropic modeling predictions and experimental results for the linear elastic dynamic regime for which the model is applicable. Therefore, isotropy of the foam is here assumed although the model is easily amenable to full orthotropic characteristics of the foam layer.

To derive the Euler–Lagrange equations of motion for the coupled system, strain–displacement relations must be assumed for each layer. Continuity of displacement is applied between the poroelastic spring (thick plate) and the bounding thin plates. This allows for the displacements of the poroelastic spring to be expressed in terms of the displacements of the base and top plates. The number of unknowns to compute is therefore reduced to just the displacement responses of the base and top plates. Given that the base and top plates are assumed to be thin, by Love–Kirchhoff assumptions only two unknowns need to be computed: $w(x,y,t)$ and $w_m(x,y,t)$, the transverse (out-of-plane) displacements of the base and top plates, respectively.

Next, a Ritz method solution is assumed for the two unknowns. In this work, a hierarchical trigonometric function set is employed for the trial functions [33].

$$w(x,y,t) = \sum_{n=1}^{N} a_n(t)\phi_n(x,y) \tag{1}$$

$$w_m(x,y,t) = \sum_{r=1}^{R} c_r(t)\psi_r(x,y) \tag{2}$$

In Eqs. (1) and 2, $a(t)$ and $c(t)$ are the generalized coordinates of the base and top plates, respectively; $\phi(x,y)$ and $\psi(x,y)$ are the assumed trial functions; and N and R are the number of modes taken in the Ritz expansions.

Finally, assuming harmonic time response of the system and substituting the Ritz expansions for the two unknowns into the Euler–Lagrange equations, the governing equations of motion for the system are determined to be

$$\left\{\begin{bmatrix}\mathbf{K}_m+\mathbf{K}_{s,\text{top}} & \tilde{\mathbf{K}}_{s,\text{base}}\\ \tilde{\mathbf{K}}_{s,\text{top}} & \mathbf{K}+\mathbf{K}_{s,\text{base}}\end{bmatrix}+j\omega\begin{bmatrix}\mathbf{C}_m+\mathbf{C}_{s,\text{top}} & \tilde{\mathbf{C}}_{s,\text{base}}\\ \tilde{\mathbf{C}}_{s,\text{top}} & \mathbf{C}+\mathbf{C}_{s,\text{base}}\end{bmatrix}-\omega^2\begin{bmatrix}\mathbf{M}_m+\mathbf{M}_{s,\text{top}} & \tilde{\mathbf{M}}_{s,\text{base}}\\ \tilde{\mathbf{M}}_{s,\text{top}} & \mathbf{M}+\mathbf{M}_{s,\text{base}}\end{bmatrix}\right\}\begin{bmatrix}\mathbf{c}(\omega)\\ \mathbf{a}(\omega)\end{bmatrix}=\begin{bmatrix}\mathbf{0}\\ \mathbf{F}(\omega)\end{bmatrix} \tag{3}$$

where $\mathbf{K}$, $\mathbf{C}$ and $\mathbf{M}$ are the stiffness, damping and mass matrices, respectively; subscript m refers to those of the mass layer; subscript s refers to those components due to the spring layer written in terms either of the (subscript) base or top plate displacements; the terms having a $\tilde{}$ indicate elastic coupling terms stemming from application of continuity between the spring layer and the bounding plates; matrix terms without subscripts refer to the host plate components; and ω is the circular frequency of excitation. At present, the damping is assumed to be proportional to the mass and stiffness matrices such that

$$\mathbf{C} = \alpha\mathbf{M}+\beta\mathbf{K} \tag{4}$$

where α is the mass-proportional damping constant (units radians/s) and β is the stiffness-proportional damping constant (units s/radians). Given the low frequency range of interest, only stiffness-proportional damping is considered with the further assumption that $\beta=\eta/\omega$ where η is the isotropic loss factor of the layer.

The generalized forces, $\mathbf{F}$, are computed by the evaluation of the base plate trial functions at the location of the applied point forces

$$\mathbf{F}(\omega) = \sum_{n=1}^{N}\sum_{i=1}^{N_f}\phi_n(x_i^f,y_i^f)f_i(\omega) \tag{5}$$

where N_f is the number of applied forces, f_i, at locations (x_i^f,y_i^f).

In the present study, the coupled governing equations, Eq. (3), are solved over a range of frequencies, ω, and the base plate and top plate out-of-plane vibration response may be predicted from reconstruction of the responses using the assumed Ritz expansion solutions, Eqs. (1) and (2), at a location (x,y). By assumption of harmonic response, the velocity and acceleration of the plates may be computed by the relations: $\dot{w}(x,y,\omega)=j\omega[w(x,y,\omega)]$ and $\ddot{w}(x,y,\omega)=-\omega^2[w(x,y,\omega)]$. Additional response metrics may be computed—spatial-average mean-square velocity, sound radiation, etc.—and the derivations for these useful metrics may be found in Ref. [26].

3. Description of shaker experiment

An assessment of the validity of the model may be carried out by studying the accuracy of the predicted SDOF resonant dynamics which are of greatest importance from a vibration control perspective. These dynamics are most prevalent when the devices are excited only by transverse vibration, inducing rigid-body motion of the mass layer over the poroelastic spring, and therefore a shaker platform experiment is the most applicable scenario to study.

Fig. 3 shows a schematic of the laboratory test conducted: a poroelastic DVA sample is attached to a stiff shaker platform which is excited by white noise. A laser vibrometer measures the velocity of the DVA top plate while an

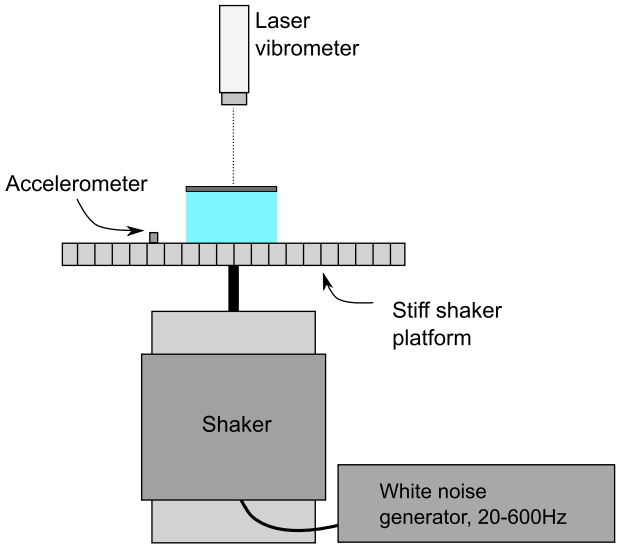

Fig. 3. Schematic of the shaker table test to measure SDOF resonance characteristics of the foam DVAs.

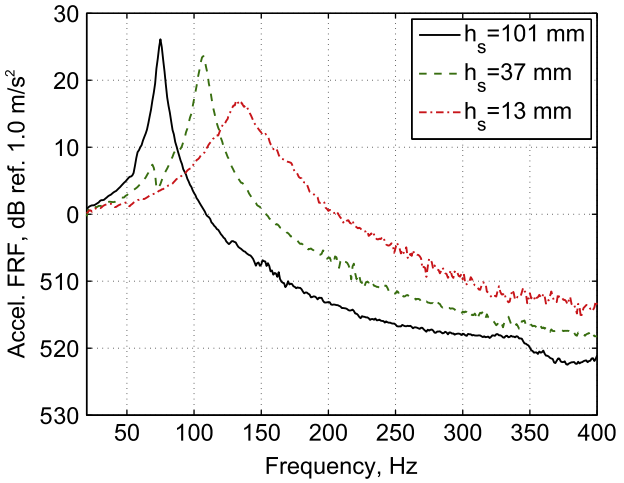

Fig. 4. Sample variation of the resonance frequency and damping of foam DVA (device 1) as the foam spring thickness is varied.

accelerometer measures the base platform acceleration. The acceleration frequency response function (FRF) is computed as the ratio of the top plate acceleration to the base plate acceleration. Since the DVA top mass oscillates in rigid body translation at resonance, compressing and stretching the foam beneath, the frequency response of a DVA on a shaker table will ideally appear identical to that of a 1DOF vibration absorber. Fig. 4 presents experimental results from a DVA as the thickness of the poroelastic layer was reduced from 101 mm to 13 mm, showing the increase in both resonance frequency and damping as the thickness is reduced.

To compare the model output of this resonance dynamic, the base plate and top plate are both considered to have free boundary conditions. The base plate is assumed to be exceptionally rigid as compared to the stiffness of the top plate. The foam used experimentally was melamine foam, Willtec©, manufactured by Pinta Acoustic, Inc. To attach the mass layers to the foam, a very thin layer of spray glue is applied to the mass which is thereafter placed onto the foam. Geometric and mechanical properties used in the test and model for the layers are provided in Table 1.

Values of Young's modulus E, Poisson's ratio ν, and loss factor η of the melamine foam were determined using an iterative routine of comparison amongst published data, present experimental results, and the resulting model predictions. First, observation was made of the range of parameters given in literature [26,29,31] and a choice of the necessary elastic parameters within the range were taken as initial input to the model. Next, experimental data was acquired of the resonance frequency and damping of the DVA samples having thickness $h_s > 40$ mm and compared against modeling predictions. The elastic parameters were then iteratively updated until the modeled results were in good agreement with experimental data. This method assumes that the elastic parameters of the foam are isotropic and linear, and it was the

Table 1
Geometric and mechanical properties of the layers.

Layer	a (mm)	b (mm)	h (mm)	E (Pa)	v	ρ (kg/m^3)	η
Base	300	150	10	1e14	0.1	300	0.001
Mass 1	75	50	1.498	2.1e11	0.33	7800	0.001
Mass 2	75	50	0.6096	2.1e11	0.33	7100	0.001
Foam	75	50	–	1.1e5	0.4	8	0.07

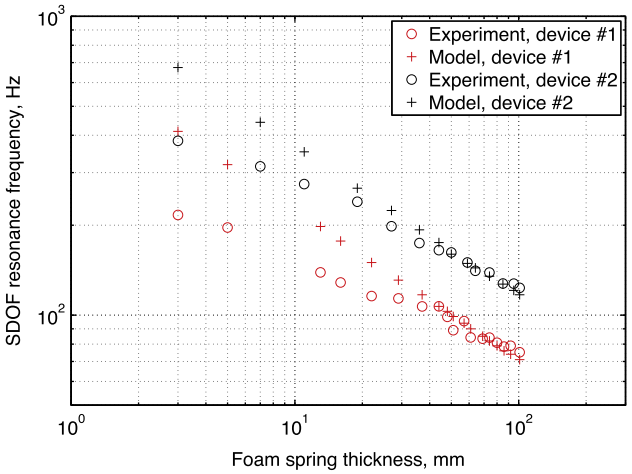

Fig. 5. Predicted and measured natural frequencies of the foam DVA samples.

aim of the present work to determine to what extent such modeling assumptions continue to yield accurate estimates of the poroelastic DVA response as the foam thickness is modified.

The measurement point of the velocity of the top mass layer was at the center of the top plate: $(x,y)=(0,0)$ mm. The measurement point of the acceleration of the base plate was slightly off center in the y-axis: $(x,y)=(0,-30)$ mm. The thickness of the poroelastic spring layer is modified with each run of the model to observe the parameter's influence on the resonance frequency. In practice, changes in the foam thickness were achieved using a bandsaw. Cutting poroelastic materials proved to be challenging and many samples were required since a number were torn by the bandsaw blade. No single blade selection and speed seemed amenable for all required cuts as it generally became more difficult to consistently cut the foam as the thickness was significantly reduced.

In evaluating the influence of a mass layer dynamically interacting with a poroelastic material, care must be taken to avoid interfering influences in the investigation. Ref. [34] determined numerous interactions existing between a dynamic mass inclusion (or layer) and poroelastic material. Not only the thickness of the foam between the mass and vibrating structure plays a role in determining the natural frequency of the sample, but also features related to the planar range of foam around the mass, the shape of the mass, and the potential existence of other masses in close proximity. To strictly determine the influence foam thickness on the DVA natural frequency and damping, it is necessary to hold constant these additional parameters from test to test. As such, the mass layer fully covered the foam sample and the length-width dimensions of the sample remained constant for all tests: only melamine foam thickness was modified between evaluations. This protocol eliminates extraneous influences in the experimental results, allowing for the accurate determination of the relation between foam thickness and DVA resonance characteristics.

4. Experimental and model comparison

4.1. Comparison of SDOF resonance frequency

Fig. 5 plots the comparison between the modeled and measured SDOF natural frequency of the poroelastic DVAs for two samples having unique mass layers, device 1 being more than twice the mass of device 2. For poroelastic thicknesses of $h_s > 30$ mm, the model is in good agreement with measurements, accurately tracking the variation of the resonance frequency. However, for thinner foam layers, measurements show a steady reduction in the natural frequency as compared with the linear elastic predictions of the model. This indicates that for thinner foam layers there is a softening effect of the equivalent transverse stiffness of the poroelastic spring.

Explanation and validation of this effect is given in past literature on the nonlinear and viscoelastic characteristics of poroelastic foams due to varying levels of static or dynamic compression [29,30,32]. For low compression levels, the elastic

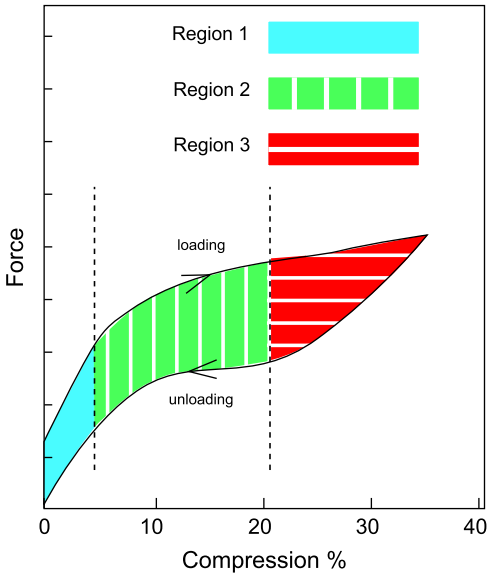

Fig. 6. Force–deflection curve for poroelastic foams with small hysteresis for loading/unloading; derived from Fig. 1 in Ref. [29].

dynamics of melamine foams are linear, Region 1 in Fig. 6, derived from Fig. 1 in Ref. [29]. However, for moderate compression levels, Region 2, the foam undergoes a softening effect. At extreme compression levels, Region 3, the foam exhibits hardening spring characteristics prior to cell collapse or tearing. Similar trends are observed for polyurethane foams [30].

It is noted that the present DVA configuration and test setup is conceptually identical to the uniaxial compression protocol used to determine stiffness parameters of melamine foam [29] and to determine the relationship of Fig. 6. The controlled test utilizes a shaker compressing a rectangular prism of poroelastic material between two plate layers; the imposed static and oscillating displacements of a moving plate strain the foam due to the opposing fixed plate. Poisson's effect strain and force through the foam are measured so as to back-calculate Young's modulus and Poisson's ratio from a three-dimensional FE code [29]. In comparison to the test protocol, the present evaluation utilizes the resonance of one plate (the DVA top mass layer) as the dynamic testing plane. As such, we anticipate that experimental results of the present work to demonstrate stress–strain relationships similar to the empirical evaluations from the testing protocol.

In the context of the present DVA study, the net dynamic compression of the full foam thickness is negligible for thick poroelastic foam springs. The mass layer oscillates in one-dimensional rigid-body motion alternatively compressing and stretching the melamine foam to a minor extent. Indeed, for the masses chosen in the present tests, the oscillation of the top mass layer is nearly imperceptible even for high shaker platform accelerations of 2 g (19.6 m/s^2). However, as the thickness of the foam layer is reduced, the net compression and extension of the foam spring increases and the transverse stiffness of the spring is effectively reduced. This explains the model's overestimation of the predicted natural frequencies of the devices in Fig. 5 for thinner foam layers.

It is interesting to note that a comparative experiment was performed in the work deriving the model used in this study, Ref. [26], but the opposite effect was observed in the experiments: a hardening spring effect as the foam thickness was reduced. This contradicts earlier literature [29,30,32] and the present experiments.

In Fig. 5, as the foam thickness is reduced device 1 appears to more plainly exhibit the softening spring effect before device 2. This is explained by the fact that device 1 is resonating at lower frequencies since it uses a mass layer of greater area density (kg/m^2) than device 2. Thus there is greater transverse oscillation amplitude of the device 1 mass and therefore greater dynamic compression of the foam spring, inducing the onset of the softening spring effect prior to its appearance for the device 2 sample.

Recall that the model employs not only linear stress–strain relationships for the poroelastic material but its present implementation utilizes isotropic assumptions for the foam layer. Anisotropic effects are anticipated to be more influential for thin melamine foam samples where the pore dimension approaches the order of the sample thickness [35]. In this case, the continuum domain assumptions of the model would misrepresent the problem studied. The results of Fig. 5 show that the isotropic and linear assumptions of the model do not inhibit accurate predictions of the DVA natural frequency for thicker foam samples. Only once the melamine foam thickness is reduced to approximately $h_s < 30$ mm do the predictions begin to adversely deviate from experimental results. In this range both softening spring and anisotropic influences are presumed to become more dominant. However, at the lower natural frequencies, < 200 Hz, for which the DVAs are of greatest use in a vibration control context, the model lends useful and reasonably accurate predictions of the DVA natural frequency.

4.2. Comparison of damping at the SDOF resonance

The benefit of poroelastic foam to serve as the distributed spring layer of the present DVA is twofold: achieving low natural frequencies with ease and the inherent hysteric damping induced as the foam layer is compressed and stretched by the top mass layer at resonance. However, linear elasticity assumptions in the model consider the loss factor, η, of the foam to be a constant regardless of the thickness of the foam material. In the model in Section 3, Table 1 shows that a loss factor of $\eta = 0.07$ was used in all predictions of the SDOF resonance of the devices, which was the parameter that yielded closest agreement to the measured samples having thicker foam springs, $h_s > 40$ mm. In Fig. 4, reduction in the foam thickness yields a gradual increase in the damping at resonance which is otherwise not accounted for in the model.

To approximate the experimentally observed loss factor, a curve-fitting procedure may be utilized. Consider the distributed DVA to be equivalent to a SDOF mass–spring–damper excited near resonance. The classical equation governing these dynamics is

$$m\ddot{x} + c\dot{x} + kx = 0 \tag{6}$$

With a loss factor model of damping, this is rewritten

$$m\ddot{x} + k(1 + j\eta)x = 0 \tag{7}$$

Taking the Laplace transform of this equation with zero initial conditions yields

$$\left[s^2 + \frac{k}{m}(1 + \mathrm{j}\eta)\right]X(s) = 0 \tag{8}$$

where $X(s)$ is the Laplace transform of $x(t)$ and s is the Laplace variable. The two roots (poles) of the polynomial in s in Eq. (8) are complex conjugates:

$$s_{1,2} = \pm \mathrm{j}\sqrt{\frac{k}{m}}\sqrt{1 + \mathrm{j}\eta} \tag{9}$$

By the binomial theorem, for $\eta \ll 1$, Eq. (9) is rewritten as

$$s_{1,2} = \pm \mathrm{j}\sqrt{\frac{k}{m}}\left(1 + \frac{1}{2}\mathrm{j}\eta\right) \tag{10}$$

From Eq. (10), the natural frequency of the DVA, ω_n (units radians/s), and the loss factor of the device, η, may be determined by the following equations:

$$\omega_n = \left|\mathrm{Imag}\{s_{1,2}\}\right| \tag{11}$$

$$\eta = 2\left|\frac{\mathrm{Real}\{s_{1,2}\}}{\mathrm{Imag}\{s_{1,2}\}}\right| \tag{12}$$

Using the experimental data from the shaker tests, a 2-pole curve fit was made to the resonant responses using the MATLAB Signal Processing Toolbox [36]. After establishing the two poles, $s_{1,2}$ (recall they are necessarily complex conjugates), the measured loss factor of the DVA for a given foam thickness was determined from Eq. (12). Fig. 7 plots the results of this procedure for the loss factor as a function of the DVA foam thickness.

The loss factor of device 1 is found to gradually increase with decreasing foam thickness. Device 2 shows a much smaller rate of increase until a sudden increase for the thinnest sample measured. The change in loss factor as a function of the poroelastic spring thickness is explained for the same reasons as the softening trend in the spring. Past work has shown that the loss factor induced by moderate dynamic compression/stretching of poroelastic materials (Region 2 from Fig. 6) is slightly increased as compared with the linear regime (Region 1) [30,32]. Device 1 exhibits this effect more gradually since a greater compression of the foam is achieved due to the heavier top mass layer than that of device 2, as earlier described in Section 4.1. Thus, the results of Fig. 7 are consistent with the past literature and further set limitations for accurate prediction of the model unless this effect is accommodated for in the implementation of DVAs having thin foam springs. Knowledge of how much compression of the foam is induced by a given DVA design could be estimated from knowledge of the SDOF resonance frequency: the lower the frequency, the more likely that a thinner poroelastic spring layer would exhibit a higher loss factor at resonance. As in the prior section, 'thinner' may be classified as $h_s < 30$ mm.

5. Remarks on modeling and experimental results

In Section 4.1 we find that the model overpredicts the effective stiffness of the poroelastic DVA as a result of reduced foam thickness. In Section 4.2 we see that the measured loss factor of the foam spring dramatically increases for thinner samples, which can only be accounted for in the model by replacement of the loss factor used in evaluation since this parameter is assumed constant.

These limitations are a result of the linear elastic, isotropic assumptions used to model a poroelastic material. Although the model is fairly accurate and therefore beneficial as a computationally efficient design tool for moderate foam thicknesses of approximately $h_s > 30$ mm, the dynamics of poroelastic materials for thinner samples become highly

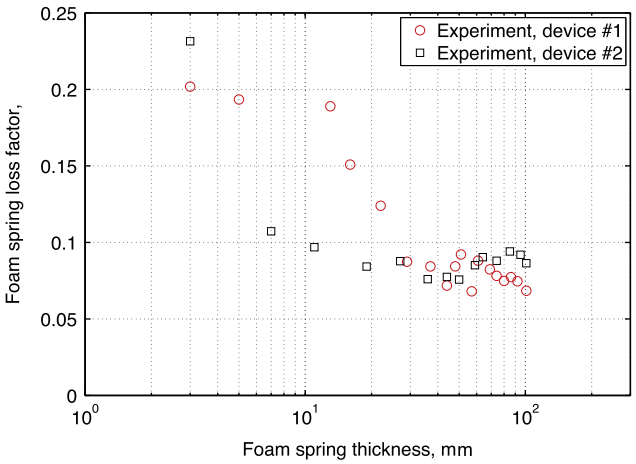

Fig. 7. Experimentally determined loss factor of the foam DVA samples for changing foam thickness.

influenced by factors not accounted for in the present analytical formulation. We see this plainly by considering the seminal Biot–Allard constitutive relationship for net stress within a poroelastic differential element [37,38]

$$\sigma_{ij} = 2G\epsilon_{ij} + \left[K - \frac{2}{3}G\right]\delta_{ij}\epsilon_{kk} - \alpha\delta_{ij}p \tag{13}$$

where σ_{ij} represents the stress tensor, ϵ_{ij} is the strain tensor, G is the shear modulus, K is the bulk modulus, and δ_{ij} is the Kronecker relationship. The last term in Eq. (13) is notably absent in the present formulation of the model evaluated in this work: the vibroacoustic component $-\alpha\delta_{ij}p$. The coupling between elastic and fluid domains is α and the acoustic pressure p is found to increase in consequence to an increase in the dynamic compression percentage of the DVA foam spring. As a result, the model neglects a component of the constitutive stress relationship for poroelastic materials whose influence becomes much more substantial for thin poroelastic layers. In light of the vibroacoustic term's role in Eq. (13), the effective stiffness of the foam spring should *reduce* for very thin samples that undergo greater dynamic compression.

This explanation conforms to the empirical findings of past work [29,30,32] and in the present data of Fig. 5. These results demonstrate that practical engineering assumptions employed to efficiently model the DVA with poroelastic spring [26] have real and observable limitations but also highlight the difficulty that would be involved in attaining a comprehensive exactness of prediction. The vibroacoustic interaction between porous frame and filling fluid of poroelastic materials is truly an ultimate challenge for researchers [39].

6. Conclusions

This work presented a summary of a computationally efficient model earlier developed to predict the coupled elastic dynamics of poroelastic distributed vibration absorbers and externally excited structural panels. The model predictions were compared against experimental data in determining the extensibility of the model in estimating the poroelastic DVA dynamics as the foam spring varied in thickness. Experimental observations were found to be in agreement with established literature on the elastic characterization of poroelastic materials for moderate dynamic compression in terms of the changing DVA resonance frequency and damping. Linear elastic and isotropic characterization of the poroelastic materials reduces the fidelity of the continuum domain model but over a range of reasonable DVA design parameters the model provides an accurate and efficient prediction of DVA resonant dynamics as compared to three-dimensional FE analysis. A limit on the modeling accuracy to melamine foam spring thicknesses of approximately $h_s > 30$ mm was observed which is regularly satisfied in achieving lower device natural frequencies, < 200 Hz, that are encountered in modal structural vibration.

Acknowledgments

The author is grateful for the enlightening interaction and comments by reviewers which aided in the development of more insightful conclusions from the study.

References

[1] H. Oberst, K. Frankenfeld, On the damping of bending vibrations on thin sheet metal by firmly bonded coatings, *Acustica* 2 (4) (1952) 181–194.
[2] E.M. Kerwin, Damping of flexural waves by a constrained viscoelastic layer, *The Journal of the Acoustical Society of America* 31 (7) (1959) 952–962.

[3] M.J. Yan, E.H. Dowell, Governing equations for vibrating constrained-layer damping sandwich plates and beams, *Journal of Applied Mechanics* 39 (4) (1972) 1041–1046.
[4] P.R. Mantena, R.F. Gibson, S.J. Hwang, Optimal constrained viscoelastic taped lengths for maximizing damping in laminated composites, *AIAA Journal* 29 (10) (1991) 1678–1685.
[5] B. Azvine, G.R. Tomlinson, R.J. Wynne, Use of active constrained-layer damping for controlling resonant vibration, *Smart Materials and Structures* 4 (1) (1995).
[6] A. Baz, J. Ro, Vibration control of plates with active constrained layer damping, *Smart Materials and Structures* 5 (1996) 272–280.
[7] L. Cremer, M. Heckl, B.A.T. Petersson, *Structure-Borne Sound*: *Structural Vibrations and Sound Radiation at Audio Frequencies*, third ed. Springer, Berlin, 2005.
[8] H. Frahm, Means for damping the rolling motion of ships, 1910. U.S. Patent #970,368.
[9] H.H. Frahm, Results of trials of the anti-rolling tanks at sea, *Journal of the American Society for Naval Engineers* 23 (2) (1911) 571–597.
[10] R. Moaleji, A.R. Greig, On the development of ship anti-roll tanks, *Ocean Engineering* 34 (1) (2007) 103–121.
[11] J.P. Den Hartog, *Mechanical Vibrations*, fourth ed. Dover Publications, New York, NY, 1985.
[12] J.C. Snowdon, Vibration of simply supported rectangular and square plates to which lumped masses and dynamic vibration absorbers are attached, *Journal of the Acoustical Society of America* 57 (3) (1975) 646–654.
[13] K. Liu, J. Lie, The damped dynamic vibration absorbers: *revisited and new result*, *Journal of Sound and Vibration* 284 (2005) 1181–1189.
[14] R.G. Jacquot, J.E. Foster, Optimal cantilever dynamic vibration absorbers, *Journal of Engineering for Industry* 99 (1977) 138–141.
[15] J.J. de Espíndola, C.A. Bavastri, E.M.O. Lopes, On the passive control of vibrations with viscoelastic dynamic absorbers of ordinary and pendulum types, *Journal of the Franklin Institute* 347 (1) (2010) 102–115.
[16] M.P. Singh, S. Singh, L.M. Moreschi, Tuned mass dampers for response control of torsional buildings, *Earthquake Engineering and Structural Dynamics* 31 (4) (2002) 749–769.
[17] L. Zuo, S.A. Nayfeh, The two-degree-of-freedom tuned-mass damper for suppression of single-mode vibration under random and harmonic excitation, *Journal of Vibration and Acoustics* 128 (2006) 56–65.
[18] S-M. Kim, S. Wang, M.J. Brennan, Dynamic analysis and optimal design of a passive and an active piezo-electrical dynamic vibration absorber, *Journal of Sound and Vibration* 330 (4) (2011) 603–614.
[19] T.L. Smith, K. Rao, I. Dyer, Attenuation of plate flexural waves by a layer of dynamic absorbers, *Noise Control Engineering Journal* 26 (2) (1986) 56–60.
[20] M.S. Khun, H.P. Lee, S.P. Lim, Structural intensity in plates with multiple discrete and distributed spring-dashpot systems, *Journal of Sound and Vibration* 276 (2004) 627–648.
[21] M.N. Hadi, Y. Arfiadi, Optimum design of absorber for mdof structures, *Journal of Structural Engineering* 124 (11) (1998) 1272–1280.
[22] M.B. Ozer, Extending den Hartog's vibration absorber technique to multi-degree-of-freedom systems, *Journal of Vibration and Acoustics* 127 (2005) 341–350.
[23] C.A. Gentry, C. Guigou, C.R. Fuller, Smart foam for applications in passive–active noise radiation control, *Journal of the Acoustical Society of America* 101 (4) (1997) 1771–1778.
[24] P. Leroy, N. Atalla, A. Berry, Three dimensional finite element modeling of smart foam, *Journal of the Acoustical Society of America* 126 (6) (2009) 2873–2885.
[25] A. Kundu, A. Berry, Active control of transmission loss with smart foams, *Journal of the Acoustical Society of America* 129 (2) (2011) 726–740.
[26] P. Marcotte, A Study of Distributed Active Vibration Absorbers (DAVA). PhD Thesis, Virginia Polytechnic Institute and State University, Blacksburg, Virginia, 2004.
[27] H. Osman, M.E. Johnson, C.R. Fuller, P. Marcotte, Interior noise reduction of composite cylinders using distributed vibration absorbers, *Proceedings of the Seventh AIAA/CEAS Aeroacoustics Conference*, Vol. 2, Maastricht, The Netherlands, 2001, pp. 2001–2230.
[28] P. Marcotte, C.R. Fuller, P. Cambou, Control of the noise radiated by a plate using a distributed active vibration absorber (dava), Active 99, *Proceedings of the International Symposium on Active Control of Sound and Vibration*, Fort Lauderdale, FL, USA, 1999, pp. 447–456.
[29] L. Jaouen, A. Renault, M. Deverge, Elastic and damping characterizations of acoustical porous materials: *available experimental methods and applications to a melamine foam*, *Applied Acoustics* 69 (2008) 1129–1140.
[30] S.W. White, S.K. Kim, A.K. Bajaj, P. Davies, D.K. Showers, P.E. Liedtke, Experimental techniques and identification of nonlinear and viscoelastic properties of flexible polyurethane foam, *Nonlinear Dynamics* 22 (2000) 281–313.
[31] A. Renault, L. Jaouen, F. Sgard, Characterization of elastic parameters of acoustical porous materials from beam bending vibrations, *Journal of Sound and Vibration* 330 (9) (2011) 1950–1963.
[32] R. Singh, P. Davies, A.K. Bajaj, Identification of nonlinear and viscoelastic properties of flexible polyurethane foam, *Nonlinear Dynamics* 34 (3) (2003) 319–346.
[33] O. Beslin, J. Nicolas, A hierarchical functions set for predicting very high order plate bending modes with any boundary conditions, *Journal of Sound and Vibration* 202 (5) (1997) 633–655.
[34] K. Idrisi, M.E. Johnson, D. Theurich, J.P. Carneal, A study on the characteristic behavior of mass inclusions added to a poro-elastic layer, *Journal of Sound and Vibration* 329 (2010) 4136–4148.
[35] R. Guastavino, P. Göransson, Vibration dynamics modeling of anisotropic porous foam materials, *Proceedings of Forum Acusticum*, Budapest Hungary, 2005, pp. 123–128.
[36] MathWorks. *MATLAB User Guide*. The MathWorks, Inc., Natick, MA, 2011.
[37] J.F. Allard, *Propagation of Sound in Porous Media. Modelling Sound Absorbing Materials*, Elsevier Applied Science, New York, NY, 1993.
[38] K. Idrisi, Heterogeneous (HG) Blankets for Improved Aircraft Interior Noise Reduction. PhD Thesis, Virginia Polytechnic Institute and State University, Blacksburg, Virginia, 2008.
[39] A. Sestieri, A. Carcaterra, Vibroacoustic: *the challenges of a mission impossible? Mechanical Systems and Signal Processing* 34 (2013) 1–18.